Chapter 5

Concluding Remarks and Future Actions

Combustion is a phenomenon with a complex mathematical formulation unfeasible to be solved with analytical solutions. Traditionally, experimental techniques have played an important role in this field. However, numerical simulation of combustion phenomena is becoming a promising and powerful tool and a very useful ingredient in the design of industrial equipment. Even though computational capabilities have increased enormously in the last decade, the numerical resolution requires large computational resources due to the inherent complexity of the phenomenon (viz. multidimensional flames considering finite rate kinetics, radiation in participating media, turbulence regimes, etc). Therefore, contributions to develop capable mathematical models reducing the complexity and the stiffness as well as efficient numerical techniques are of great importance for the technical and scientific community.

The main contribution of the present thesis is the analysis and application of the laminar flamelet concept to the numerical simulation of both laminar and turbulent flames. Assuming a one-dimensional behaviour of the combustion phenomena in the normal direction to the flame front, and taking into account an appropriate coordinates transformation, flamelet approaches reduce the complexity of the problem for the resolution of the chemistry involved.

The basic mathematical formulation and numerical tools studied and applied for the numerical simulation of chemically reactive flows are exposed in the introduction chapter and are considered as the starting point.

In Chapter 2, a co-flow partially premixed methane/air laminar flame is extensively studied by means of multidimensional numerical simulations. A parallel multiblock algorithm has been used for the numerical simulation obtaining an excellent parallel efficiency. A post-processing verification tool has been carefully applied to assess the quality of the numerical solutions. Different levels of partial premixing have been analysed from an equivalence ratio of $\Phi=\infty$ (non-premixed flame) to $\Phi=2.464$.

A comprehensive study has been performed considering different mathematical formulations and their validation process against experimental data from the literature. Firstly, chemical models from an irreversible single-step to full chemistry mechanisms have been considered. Main differences are shown in the pollutant formation prediction. Inlet boundary conditions have also been investigated. On the transport modelling approaches analysis, the formulation considering non-unity Lewis numbers has been shown to be suitable compared to detailed transport. The consideration of a unity-Lewis number notably over-predicts the maximum temperature at the centerline and the flame height. It is also shown that the Soret effect has a minor contribution. Radiant heat exchange has been shown to affect the flame temperature considerably and, consequently, the pollutant formation.

In Chapter 3, the deduction of the mathematical formulation of the flamelet equations and a deep study of the hypothesis assumed are presented. Phenomenological aspects such as the consideration of differential diffusion effects and radiation heat transfer are taken into account. The confined co-flow axisymmetric non-premixed methane/air laminar flame studied in the second chapter, is considered to apply the flamelet modelling approach. In order to validate some of the main aspects related to the flamelet mathematical approach, a comparison with the full resolution of the governing equations is performed. Steady and unsteady flamelets are compared. Aspects such as the complete set of the flamelets equations are also compared with common used simplifications of these equations. A key aspect is the modelization of the scalar dissipation rate when the flamelet equations are solved. Different possibilities have been analysed giving idea of the importance of this issue. Furthermore, when unsteady flamelets are applied, different possibilities to evaluate the flamelet lifetime are compared. Numerical solutions are also verified with the post-precessing tool employed in Chapter 2.

Steady flamelets show a proper performance to predict the main flame features when differential diffusion and radiation heat transfer are neglected. Otherwise, slow processes such as radiation or pollutant formation require unsteady flamelet modelling in order to properly capture the flame properties. Also, unsteady flamelets have been proved to be very useful in order to avoid the *super-equilibrium* effect when differential diffusion is considered. A complete flamelet equations formulation is revealed to be of great importance to correctly reproduce the main features of the flame and account for effects, i.e. the heat capacity dependence on temperature, enthalpy inter-diffusion, and differential diffusion. Furthermore, a proper modelling of the scalar dissipation rate dependence of the mixture fraction and the evaluation of the flamelet lifetime are key aspects of the flamelet simulations. If steady flamelets are considered, the use of an analytical approximation for $\chi(Z)$ is recommended, while an interactive strategy is suggested when unsteady flamelets are used. Finally, the evaluation of the Lagrangian type flamelet time has been shown to be a relevant issue when unsteady flamelets are taken into account. In general, a slight improvement of the unsteady flamelet modelling results is observed when an average velocity is used.

In Chapter 4, a characterisation of turbulence reactive flows is introduced and the laminar flamelet concept has been applied to turbulent combustion. A presumed pdf is considered to take into account the fluctuations of the mixture fraction Z and the scalar dissipation rate χ. This methodology has been applied to a piloted non-premixed methane/air turbulent flame, the so-called Flame D in the framework of the *International Workshop on Measurement and Computation of Turbulent Non-premixed Flames* (TNF) [1]. The know-how acquired in the multidimensional numerical simulation of laminar flames has been taken into account. Verified numerical results obtained with steady and unsteady flamelets are compared paying special attention to the prediction of pollutant formation. An extended version of the Eddy Dissipation Concept model is also applied and the solutions obtained are taken into account as illustrative results of the performance of simpler and widely used models.

A clear improvement in the prediction of slow processes such as radiation and pollutant formation (CO and NO_x) is shown when the transient term in the flamelet equations is retained. The numerical results obtained for this turbulent flame confirms that the averaged molecular diffusion terms that appear in the governing equations are negligible compared to the turbulent fluxes. This conclusion can be deduced for both EDC and flamelet modelling simulations. On the other hand, and as it was expected, radiation heat transfer is revealed as a key aspect to properly define the thermal level and, consequently, the temperature-dependent species such as NO_x. Finally, it is shown that the consideration of the round-jet anomaly in the turbulent model is of significant importance to estimate the position of the flame front.

In conclusion, flamelet modelling simulations are revealed to be an interesting and accurate approach for the numerical simulation of laminar and turbulent flames. Detailed chemistry can be taken into account and the inherent stiffness of the chemistry term is solved in a pre-processing task. Thus, pollutant formation such as CO and NO_x can be considered and accurately solved with flamelet models when the transient term in the flamelet equations is retained.

Future Actions

Flamelet modelling approaches discussed in this thesis would need further research to better predict the flame characteristics for multidimensional numerical simulations. The Lagrangian Flamelet Model taking into account more in-situ key information would be a research line to follow. A further study on the evaluation of the Lagrangian type flamelet time will be performed since the numerical results are found to be sensitive to the methodology employed. In addition, a full introduction of the convective terms would be of interest. Moreover, the scalar dissipation rate dependence on the mixture fraction is still an open field and contributions on this area are expected. Unsteady events such as extinction and re-ignition are key aspects for some industrial equipment, and are also of our interest.

A verification of flamelet libraries would be important to provide a criteria on the sensitivity of the simulation to the computational model parameters that account for the discretization. The verification technique employed for the CFD simulations would be a suitable candidate. In the present thesis, flamelet libraries are calculated discretizing the flamelet equations in the mixture fraction space Z and introducing a discrete number of scalar dissipation rate profiles $\chi(Z)$. This profile can be provided, among others, with any of the criteria exposed in the thesis (see section 3.2.3). The number of nodes in the Z space and the discrete number of scalar dissipation rate profiles have been chosen with a previous asymptotic study, taking into account the global behaviour of the flamelet library generation.

Flamelet models for premixed flames using the G-equation would be a further step. Flamelet models have been applied for non-premixed flames considering that the mixing process is described by the conserved scalar Z (the mixture fraction). An analogous methodology can be considered for premixed combustion taking into account another conserved scalar. For premixed combustion, flamelet models are either based on the progress variable c (defined as a normalised or reduced temperature, or normalised or reduced product mass fraction) or, more recently, on the level set approach using the scalar G. A transport equation defining a G-equation can be derived from the kinematic balance among the flow velocity, the burning velocity normal to the flame front and the front flame propagating velocity [2]. G-field, whose level represents the flame surface, is introduced to simulate the propagation of fronts. Furthermore, partially premixed flames also require an analysis and a specific modelization. See [2] for further details.

A deep understanding of soot formation constitute a challenge for scientists and engineers. Soot formation is a key aspect for a clean design of technical equipment such as engines, boilers, furnaces, etc. First, an accurate study of this phenomenon for the numerical simulations of laminar flames using the full resolution of the transport governing equations is considered of capital importance. Secondly, soot models are expected to be used with the laminar flamelet concept for numerical simulation of both laminar and specially turbulent flames. See [3–7] for further information.

Radiation heat transfer with advanced models is also in our research purposes. In the present thesis, radiation has been taken into account considering an optically thin model. This simplified model assumes that each radiation point has an unimpeded isotropic view of the cold surroundings, considered as a black body. The definition of an optically thin gas establishes that self-absorption is negligible compared to emission. In order to overcome this limitation, a complete resolution of the Radiation Transfer Equation (RTE) is required considering emission, absorption and scattering terms. The Discrete Ordinates Method (DOM) or finite volume technique are suitable for this resolution. The application of these methods for combustion systems is suggested. See [8] for further details.

Turbulence modelling of combustion systems requires further research. Referring to RANS models for numerical simulation of turbulent flames, low-Reynolds number eddy-viscosity two-equation models should be studied as well as more advanced models, i.e. non-linear eddy-viscosity models and explicit Algebraic Reynolds Stress Models (EARSM). The use of other variables, i.e. ω, to describe the dissipation of the turbulent kinetic energy is also suggested. In the mid-term run, Large Eddy Simulation (LES) of combustion systems will be applied. LES models can be more general and accurate than RANS models. Given the full time integration, phenomena such as extinction or re-ignition are more suitable to be solved with LES models. In addition, situations where the desirable time scales separation is not accomplished (fluctuating behaviour of the variables and the time-scales related to the main flow unsteady behaviour), are candidate problems for LES. In the long term run, Direct Numerical Simulations (DNS) will be attractive to simulate certain combustion flames in order to study fundamental aspects and to extract key modelling information to feed RANS and LES models. See [9–11] for further information.

In the present thesis, a piloted non-premixed methane/air turbulent flame (Flame D) has been selected as a test case given its simple flow structure without any solid. However, *complex turbulent flow structure flames* such as bluff-body flames or swirling flames would also be of great importance for the basic combustion research. Both flames, as well as Flame D, are studied in the framework of the *International Workshop on Measurement and Computation of Turbulent Non-premixed Flames* (TNF) [1]. Lifted flames would also be of great interest.

Experimental measurements of combustion systems are also a purpose in the near future research activity. An experimental set-up recently designed and constructed at CTTC will be used to measure the co-flow partially premixed methane/air laminar flame numerically studied in Chapters 2 and 3. In fact, preliminary results for temperature measurements using 50, 75 and 125 μm diameter type R (Pt-Pt/13% Rh) thermocouple-wire pairs are already available. A mass spectrometry will be used for measurements of several major species concentrations. In addition, the velocity field will be measured using the PIV (Particle Image Velocimetry) technique. Equipments for both PIV and mass spectrometry are already available at CTTC.

Other work on combustion research would be to apply the numerical infrastructure developed at the CTTC for the design of industrial combustion systems. The study of acoustics in combustion systems would also be an interesting issue. The design of domestic equipment, i.e. boilers, requires a reduction of the noise produced by combustion systems in order to improve the quality of life.

References

[1] TNF Workshop, http://www.ca.sandia.gov/TNF.

[2] N. Peters. *Turbulent combustion.* Cambridge University Press, 2000.

[3] H. Bockhorn. *Soot formation in combustion. Mechanism and models.* Kluwer Academic Publishers, 1994.

[4] A. Dederich. *Flamelet Modelling of soot formation in diffusion flames.* PhD thesis, Lund Institute of Technology, 2004.

[5] L. Wang. *Detailed chemistry, soot, and radiation calculations in turbulent reacting flows.* PhD thesis, Pennsylvania State University, 2004.

[6] Ian M Kennedy, C YAM, D.R. Rapp, and R.J. Santoro. Modeling and measurements of soot and species in a laminar diffusion flame. *Combustion and Flame*, 107:368–382, 1996.

[7] Ian M. Kennedy. Models of soot formation and oxidation. *Progress in Energy and Combustion Science*, 23:95–132, 1997.

[8] M.F. Modest. *Radiative heat transfer.* McGraw-Hill, 1993.

[9] S.B. Pope. *Turbulent Flows.* Cambridge University Press, 2000.

[10] P. Sagaut and M. Germano. *Large Eddy Simulation for Incompressible Flows.* Springer-Berlag, 2001.

[11] T. Poinsot and D. Veynante. *Theoretical and Numerical Combustion.* R.T. Edwards, Inc., 2001.

Appendix A

Flamelet libraries analysis

Chapter 3 and 4 of the present thesis are devoted to analyse the application of the flamelet modelling approach to the numerical simulation of laminar and turbulent multidimensional non-premixed flames. Numerical simulation of these combustion systems using flamelet modelling approaches requires, in a pre-processing task, the solution of flamelet equations. Therefore, given a chemical model and appropriate boundary conditions for both fuel and oxidizer streams, flamelet equations are solved and the numerical results are stored in the so-called *flamelet libraries*.

This appendix analyses the flamelet libraries taking into account some aspects also considered in Chapter 3: mathematical formulation using both sets of flamelet equations, complete (CE) and simplified (SE) forms (see section 3.2.2), and the modelization of the scalar dissipation rate dependence of the mixture fraction χ_1 and χ_2, both parametrised by the scalar dissipation rate at stoichiometric conditions χ_{st} (see section 3.2.3). The present study is restricted to the **steady flamelet** modelling approach SF.

The influence of including differential diffusion and radiation is also analysed. Four phenomenological situations are identified: i) Unity-Lewis numbers and radiation not included; ii) Unity-Lewis numbers and radiation included; iii) Fixed-Lewis numbers and radiation not included; iv) Fixed-Lewis numbers and radiation included. Differential diffusion is included fixing a constant Lewis number for each species. Radiation heat transfer is included adopting an optically thin radiation model (OTM) [1–3]. See section 3.3.2 for details.

Chemical model and boundary conditions

The selected configuration of the flamelet library is required for the test case described in Chapters 2 and 3, which is a confined co-flow axisymmetric non-premixed methane/air laminar flame. Therefore, flamelet libraries construction is hereafter analysed for a two feed system of a non-premixed flame with both stream temperatures of $298K$. The fuel stream (Z=1) has a unity methane mass fraction (Y_{CH_4}=1) and the oxidizer stream (Z=0) is of "regular" air (Y_{O_2}=0.232 and Y_{N_2}=0.768). Thus, the mixture fraction at stoichiometric conditions is Z_{st}=0.055. The detailed chemical mechanism GRI-Mech 3.0 [4] is considered.

Flamelet libraries analysis

Discussion is supported by figures A.1-A.4 and table A.1. All figures represent temperature profiles along the mixture fraction space for different conditions. The equilibrium temperature profile calculated by the STANJAN [5] is included in all the figures. Using the complete flamelet equations CE and the analytical scalar dissipation rate modelling χ_1, figure A.1 shows the temperature profile for a wide range of scalar dissipation rates at stoichiometric conditions from 2x10^{-4} to 10 and for all the phenomenological situations identified above. Figures A.2, A.3 and A.4 show temperature profiles for different model approaches and for χ_{st}=2x10^{-4}, χ_{st}=0.1 and χ_{st}=1 respectively. These figures include profiles for the complete flamelet equations CE and for both scalar dissipation rate modelling approaches χ_1 and χ_2 and, finally, the simplified flamelet equations SE with the analytical approach χ_1 for the scalar dissipation rate modelling. Also, the phenomenological situations identified above are given here with the exception of figure A.2 where only adiabatic flame conditions are plotted for the reasons exposed below.

Figures A.2-A.4 show that the omission of the term that involves the Z-derivative of the heat capacity in the flamelet equations SE produces a low temperature profile for both adiabatic and radiating flamelets.

Adiabatic flamelets

In figure A.1, temperature flamelet profiles for the complete equations formulation CE and the analytical modelling of the scalar dissipation rate χ_1 are compared for different χ_{st}. In figure A.1a, the unity-Lewis number assumption is applied and an asymptotic behaviour to the equilibrium state is observed when $\chi_{st} \to 0$.

On the contrary, when differential diffusion is considered (Fig. A.1b), this asymptotic behaviour is not found, observing an increase and a displacement of the maximum peak temperature in comparison with the equilibrium state ($\chi_{st} = 0$). For χ_{st}=2x10^{-4}, the difference between the peak temperature and the peak of the equilibrium state is more than 100 K. For the equilibrium state, and also for unity-Lewis number assumption, this temperature peak is at $Z \simeq 0.0565$ (which is close to the stoichiometric value), while the inclusion of differential diffusion produces a peak at $Z \simeq 0.0426$. This effect, so-called *super-equilibrium* [6, 7], is more evident as χ_{st} decreases (see Fig. A.1b). The responsible term of this significant displacement and this increase of temperature, is the derivative of the scalar dissipation rate with the mixture fraction ($\frac{\partial \rho \chi}{\partial Z}$) that appears in the complete formulation (CE). This effect has been shown to be more relevant for low scalar dissipation rates. Models with simpli-

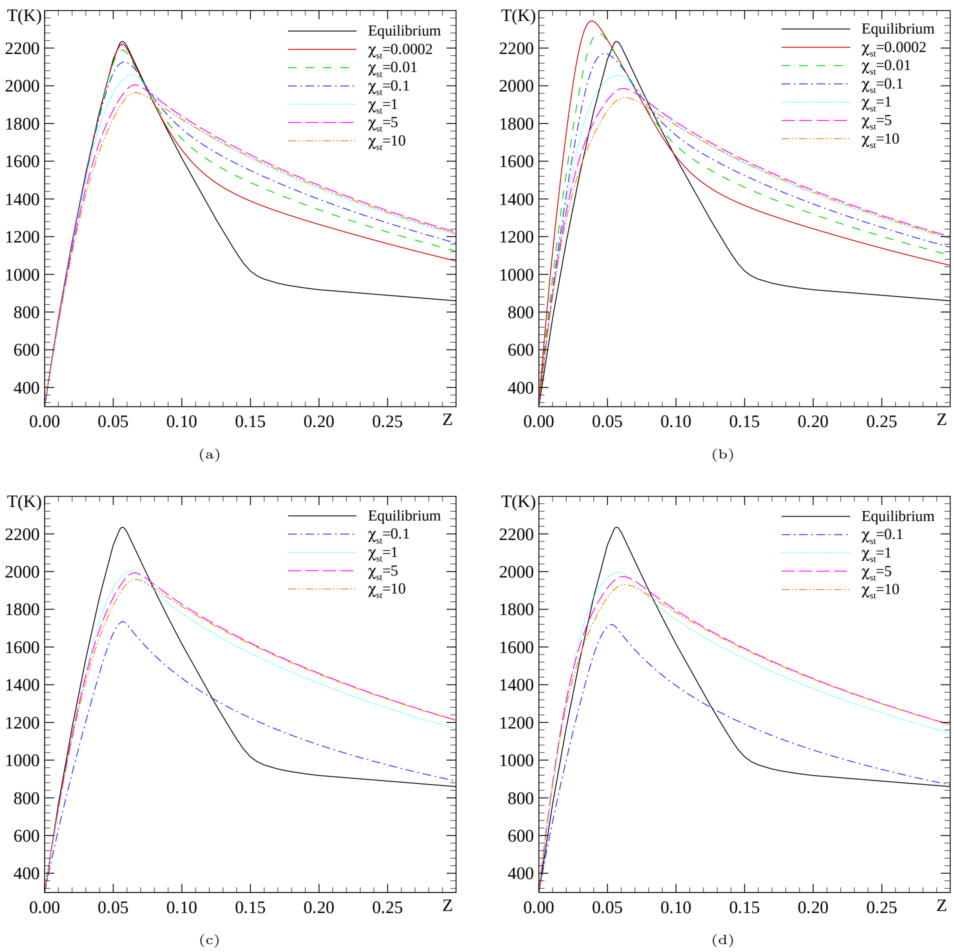

Figure A.1: Temperature flamelet profiles for different χ_{st}. Complete flamelet equations (CE) and analytical scalar dissipation rate modelling (χ_1). (a) Unity-Lewis and No-radiation; (b) Fixed-Lewis and No-radiation; (c) Unity-Lewis and radiation; (d) Fixed-Lewis and radiation.

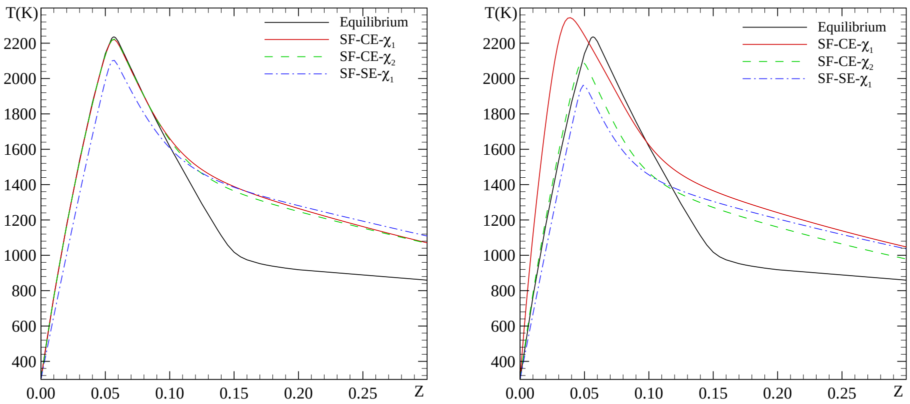

(a) (b)

Figure A.2: Temperature flamelet profiles. $\chi_{st} = 2\text{x}10^{-4}$. (a) Unity-Lewis and No-radiation; (b) Fixed-Lewis and No-radiation.

fied equations (SE) does not include this term and when the complete equations (CE) are employed with χ_2, this term is not active because each discrete value of χ_{st} is considered constant with Z. Consequently, when differential diffusion is considered, the differences of the three analysed models increase.

Radiating flamelets

Some authors argue that the temperature field predicted by the laminar flamelet model considering radiation is unrealistic [7, 8]. Bray and Peters [9] argued that radiation heat loss in a laminar flamelet is very different from radiation heat loss in an actual flame. When radiation heat loss is considered in a laminar flamelet, it implies that the radiation heat exchange occurs as thin gas radiative emissions to the surroundings within a thin region of high temperature. Also, local properties as well as global effects arising from properties at distant locations influence the flame. In calculating large scale flames (e.g. furnaces), emission and re-absorption over much larger length scales must be taken into account. Then, the optically thin model exposed in section 1.3.4 is not adequate. However, the radiative term in flamelet equations is not suitable to include re-absorption radiation effects. Bray and Peters [9] indicated the possibility to employ an enthalpy defect. Marracino and Lentini [10] successfully implement this approach. This technique is beyond the scope of this thesis since the flames studied are small enough and are commonly reported in the

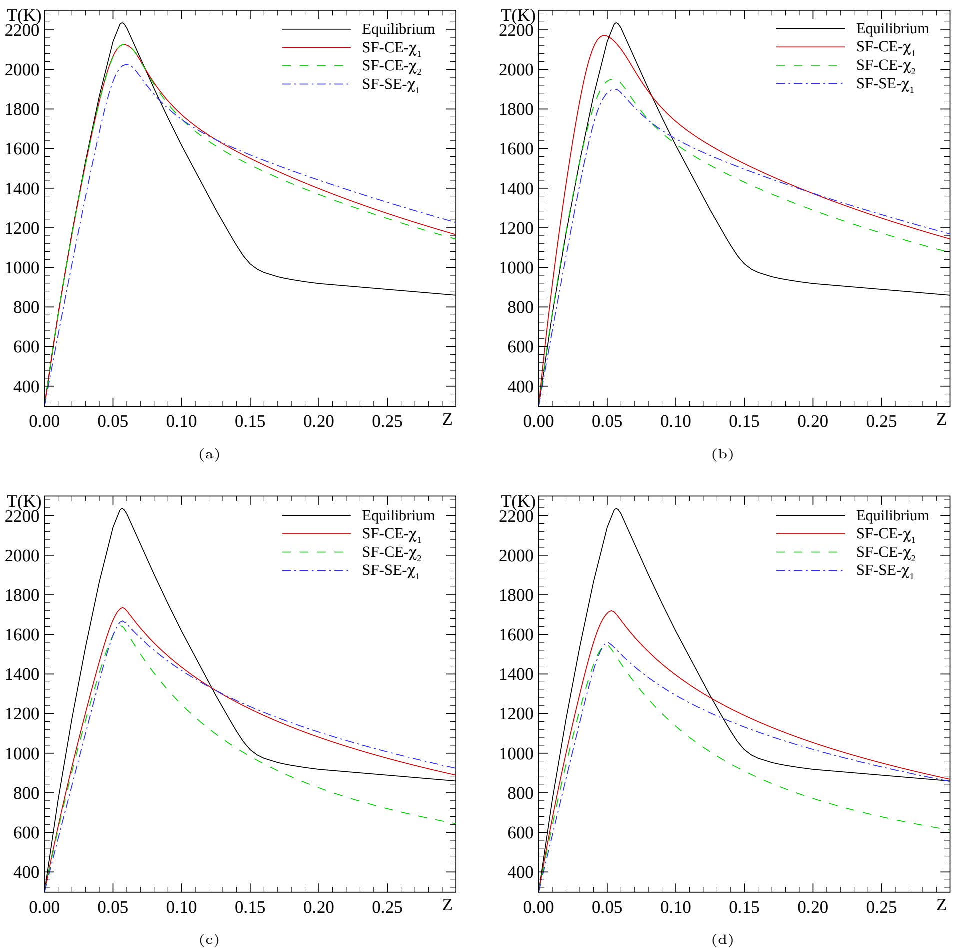

Figure A.3: Temperature flamelet profiles. $\chi_{st} = 0.1$. (a) Unity-Lewis and No-radiation; (b) Fixed-Lewis and No-radiation; (c) Unity-Lewis and radiation; (d) Fixed-Lewis and radiation.

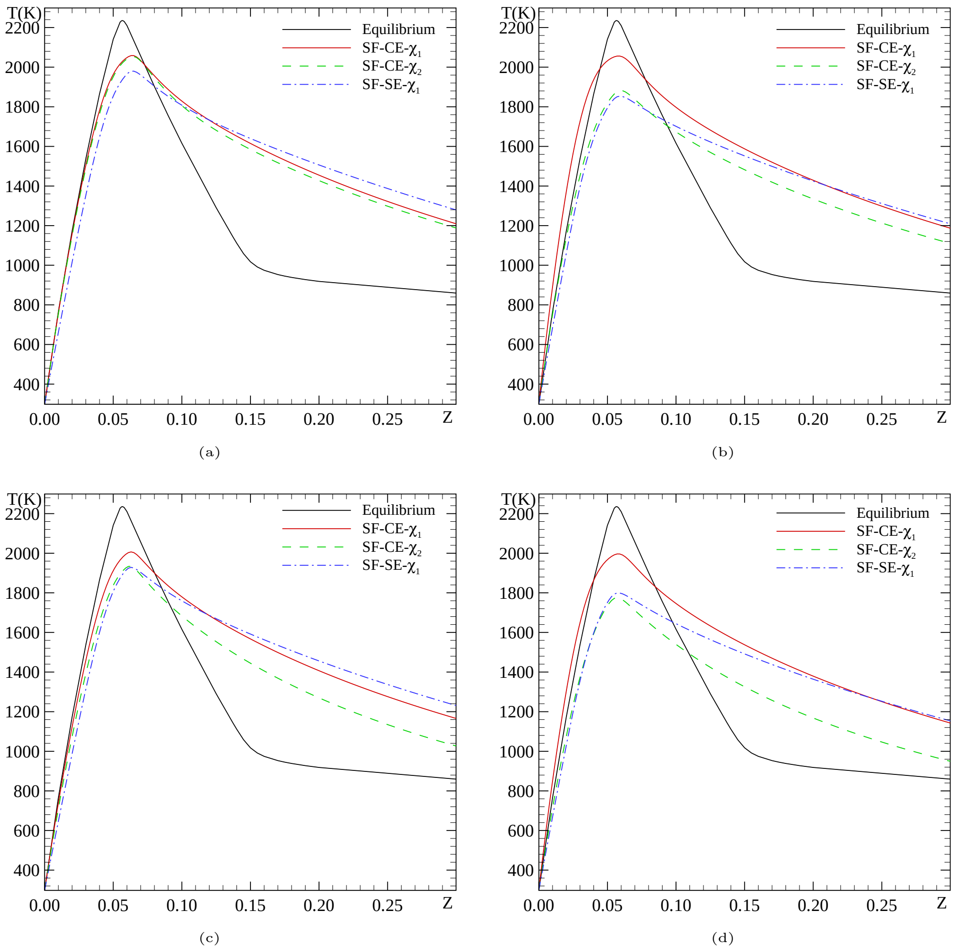

Figure A.4: Temperature flamelet profiles. $\chi_{st} = 1$. (a) Unity-Lewis and No-radiation; (b) Fixed-Lewis and No-radiation; (c) Unity-Lewis and radiation; (d) Fixed-Lewis and radiation.

literature using the optically thin model.

Flame radiation can induce another extinction limit at low scalar dissipation rates, which is in addition to the well-known extinction limit caused by the over-stretching of the flame at high scalar dissipation rates [11, 12]. At high dissipation rates, the high stretching in the flame causes high diffusion rates of species, and more fuel and oxygen penetrate each other, which leads to an incomplete reaction.

A significant decrease of the temperature profile is observed in figure A.1-bottom for both unity-Lewis and Fixed-Lewis cases, specially for low scalar dissipation rates. Figure A.1 shows that for radiation flamelets the peak temperature for $\chi_{st} = 0.1$ is approximately 500 K lower than the equilibrium state for both unity-Lewis and Fixed-Lewis considerations. In these two cases, the profiles for lower χ_{st} are not plotted since the extinction limit for low scalar dissipation rates takes place. This is also the reason why in Fig. A.2 only adiabatic flamelets are shown.

Figures A.3 and A.4 show that, when radiation is included, the use of χ_2 produces a very low temperature profile for $Z > Z_{st}$.

Extinction limits

A further topic of discussion is the value of the scalar dissipation rate at stoichiometric conditions $\chi_{st,q}$ at extinction. Table A.1 shows the extinction limit at high scalar dissipation rates for different conditions. The flamelet model used to build the flamelet libraries can have a great impact on this value. This effect seems to be more significant when differential diffusion is considered. For instance, when the complete equations CE are considered, the stoichiometric scalar dissipation rate at extinction is approximately 15 for both χ_1 and χ_2 models, while when the simplified equations SE are taken into account this value falls significantly lower (approximately 6). For radiating flamelets and both unity-Lewis and Fixed-Lewis cases the extinction limit for low scalar dissipation rates is approximately 0.1.

Flamelet model	Unity-Lewis No-Radiation	Unity-Lewis Radiation	Fixed-Lewis No-Radiation	Fixed-Lewis Radiation
CE-χ_1	25	25	20	20
CE-χ_2	25	25	20	6
SE-χ_1	15	15	6	6

Table A.1: Approximate scalar dissipation rate at stoichiometric conditions $\chi_{st,q}$ at extinction.

References

[1] K. Claramunt, R. Cònsul, C.D. Pérez-Segarra, and A. Oliva. Multidimensional mathematical modeling and numerical investigation of co-flow partially premixed methane/air laminar flames. *Combustion and Flame*, 137:444–457, 2004.

[2] R.S. Barlow, A.N. Karpetis, and J.Y. Frank, J.H. Chen. Scalar profiles and NO formation in laminar opposed-flow partially premixed methane/air flames. *Combustion and Flame*, 127:2102–2118, 2001.

[3] S. Mazumder and M.F. Modest. Advanced nongray radiation model coupled with a CFD code for large-scale fire and combustion applications. Technical report, National Sciencie Foundation, 2001.

[4] G.P. Smith, D.M. Golden, M. Frenklach, N.W. Moriarty, B. Eiteneer, M. Goldenberg, C.T. Bowman, R.K. Hanson, S. Song, W.C. Gardiner, V.V. Lissianski, and Z. Qin. Gri-Mech 3.0, http://www.me.berkeley.edu/gri_mech/.

[5] W.C. Reynolds. The Element Potential Method for Chemical Equilibrium Analysis: Implementation in the Interactive Program STANJAN. Technical report, Stanford University, Dept. of Mechanical Engr., 1986.

[6] H. Pitsch. Unsteady flamelet modeling of differential diffusion in turbulent jet diffusion flames. *Combustion and Flame*, 123:358–374, 2000.

[7] H. Pitsch, M. Chen, and N. Peters. Unsteady flamelet modeling of turbulent hydrogen-air diffusion flames. In *Proceedings of the Twenty-Seventh Symposium (International) on Combustion*, pages 1057–1064, 1998.

[8] P.J. Coelho and N. Peters. Unsteady modelling of a piloted Methane/air jet flame based on the Eulerian particle flamelet model. *Combustion and Flame*, 124:444–465, 2001.

[9] P.A. Libby and F.A. Williams (ed.). *Turbulent Reacting Flows*. Academic Press, 1994.

[10] B. Marracino and D. Lentini. Radiation modelling in non-luminous nonpremixed turbulent flames. *Combustion Science and Technology*, 128:23–48, 1997.

[11] S.H. Chan, J.Q. Yin, and B.J. Shi. Structure and Extintion of Methane-Air Flamelet with Radiation and Detailed Chemical Kinetic Mechanism. *Combustion and Flame*, 112:445–456, 1998.

[12] N. Peters. Local Quenching due to flame stretch and non-premixed turbulent combustion. *Combustion Science and Technology*, 30:1–17, 1983.